Title
Friction Dependence on Surface Roughness for Castor Oil Lubricated NiTi Alloy Sliding on Steel

Journal
Tribology transactions, 61(6)

ISSN
1040-2004

Authors
Walters, Nicholas
Martini, Ashlie

Publication Date
2018-11-02

DOI
10.1080/10402004.2018.1520949

Walters N and Martini A (2018) "Friction Dependence on Surface Roughness for Castor Oil Lubricated NiTi Alloy Sliding on Steel", Tribology Transactions, 61, 1162.

DOI: 10.1080/10402004.2018.1520949

Friction Dependence on Surface Roughness for Castor Oil Lubricated NiTi Alloy Sliding on Steel

Nicholas Walters[1] and Ashlie Martini[1]*

1. Department of Mechanical Engineering, University of California Merced, Merced USA
* Corresponding Author: amartini@ucmerced.edu

Abstract

NiTi alloys are highly resistant to corrosion with hardness and elasticity properties suitable for bearing applications. However, lubrication of this material is still being explored since many commercial lubricants are designed to function through chemical and physical interactions with steel surfaces. Previous studies suggested castor oil as a natural lubricant for NiTi and reported friction coefficients less than 0.01, i.e. superlubricity, when sliding steel against 60NiTi (60wt.%Ni, 40wt.%Ti). Here we explore the robustness of those findings by characterizing the change in friction coefficient as a function of contact pressure and surface roughness. It is found that friction is extremely sensitive to surface roughness, such that ultra-low friction could only be achieved with surfaces having roughness less than tens of nanometers, conditions which may not be achievable in some practical bearing applications.

Keywords

Friction, Non-Ferrous Alloys, Ball Bearings

Introduction

Bearings that operate in severe conditions, such as highly corrosive environments, require bearing materials that can withstand and provide low friction and wear in those conditions. One promising material for this purpose is 60NiTi, or Nitinol 60, which is a Ni-Ti alloy containing approximately 60 wt.% Ni and 40 wt.% Ti [1]. This material has been shown to exhibit very high hardness, but also to be relatively elastic, exhibiting ten times more deflection than typical bearing steel [2-5]. Recent studies have also shown that 60NiTi has an extremely high coefficient of restitution [6]. It has therefore been identified as a promising material for both bearings in both space and terrestrial bearing applications [2-5].

60NiTi bearings operate with a lubricant and there is some concern about issues of compatibility, given the generally poor response of titanium alloys to some chemicals used in lubricants. However, studies have shown that sufficiently low friction and wear can be obtained for 60NiTi in boundary lubrication with hydrocarbon and fluorocarbon oils [3,7,8]. Recently, there have been a series of studies performed to characterize the performance of these materials with castor oil lubrication [9-11]. The motivation behind such studies is that castor oil is a "green" lubricant. Castor oil has been shown to exhibit better friction and load carrying capacity in an unformulated form than commercial oil and to have comparable wear performance to commercial oil when formulated with suitable anti-wear agent [12]. Further, studies of castor oil lubricated NiTi-steed contacts showed that so-called superlubricity, i.e. a friction coefficient of less than 0.01, can be achieved under some conditions. Specifically, a friction coefficient of 0.004 was measured for pin-on-disk contact and pressures of 280 MPa. The results were explained by tribochemical reactions which resulted in the formation of a protective tribofilm [9]. Specifically, it was proposed that the castor oil degrades to yield an interface with hexanoic acid bonded to nickel oxy-hydroxide and iron oxy-hydroxide. The electrostatic repulsive interactions between the two surfaces enable low resistance to shear and therefore lead to the observed superlubricity. However, the robustness of this ultra-low friction under different operating conditions has not yet been explored.

Here, we characterize castor oil lubricated sliding contact between a NiTi alloy ball and a 52100 steel flat under a range of speeds and pressures. Contact geometries include both ball-on-flat and a "flattened" ball which approximates pin-on-disk conditions. For the flattened ball geometry, the ball surface is polished to different degrees of roughness to explore the effect of this parameter. Findings reveal that friction under castor oil lubrication is highly sensitive to surface roughness, and that friction coefficients approaching the superlubricity regime are only achievable with very smooth surfaces.

Methods

Experiments were performed with 2.38 mm radius NiTi alloy bearing balls and flat 52100 steel disks. The NiTi alloy is designated NiTi-Hf and contains 1 atomic percent Hafnium. The exact composition by weight percent is 57.6 wt.% Ni, 39.2 wt.% Ti, and 3.2 wt.% Hf. Alloying with Hf has been shown to enable the material to endure higher stress levels and data from the literature suggests that the addition of Hf does not alter the response of the material to lubrication [13]. Rather, the addition of Hf predominantly affects processability by making the heat treatment (hardening) less sensitive to cooling rates. The steel disks were polished using silicon carbide abrasive paper and polycrystalline diamond abrasive lubricated by hexylene glycol. The average roughness of the ball and disk were measured using a white light interferometer. The contact was lubricated with commercially available castor oil.

Friction measurements were performed with unidirectional sliding. The NiTi-Hf balls were secured in a collet and loaded to 30 N on the steel disk. The steel disk was fastened to a rotary drive which was rotated at a range of angular velocities corresponding to linear sliding speeds between 2.3 and 672 mm/s. The test was run for 30 seconds at each speed. All tests were performed at room temperature in open air at a relative humidity of 47 ± 0.04%. Normal and lateral force were measured at a frequency of 100 Hz and the friction coefficient was calculated as the average value over the duration of each test.

Results

The first set of measurements was performed with an as-received NiTi-Hf ball sliding on a polished 52100 steel disk. The average roughness (R_a) of the ball and disk were 60.8 +/- 1.6 nm and 1.62 +/- 0.2 nm, respectively, where the error corresponds to the standard deviation of the measured roughness data. A 30 N load in this case corresponded to a maximum Hertz pressure of 1,665 MPa. A representative data set from one trial is shown in Figure 1a, where the speed was decreased stepwise and the friction reached steady state at each speed. The average friction coefficient at each speed is plotted as a function of the ratio of speed to pressure in Figure 1b. This representation of the data is comparable to a Stribeck curve since all tests were performed at the same load and with the same castor oil lubricant, i.e. same viscosity. The results of the three independent tests were consistent and exhibited friction decreasing from 0.09 to 0.05. These results are in contrast to those reported in Ref. [9] (also shown in Figure 1b) where the friction coefficient increased with increasing speed and reached a value as low as 0.004. Two possible explanations for this difference are the geometry, i.e. ball vs. pin, and pressure, i.e. 1,665 MPa vs. 280 MPa.

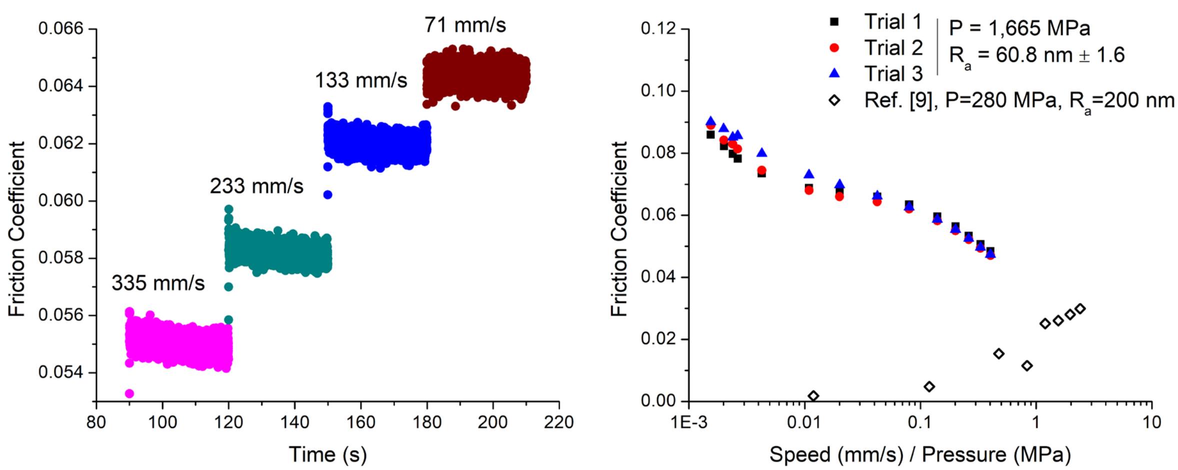

Figure 1: (a) Representative friction vs. time data from Trial 2 illustrating the test process in which the speed is decreased in a stepwise fashion (only four speeds shown for clarity). (b) Average friction at each speed for three independent tests with as-obtained NiTi-Hf *balls (solid symbols). Also shown are results obtained with a pin-on-flat geometry in Ref. [9] (hollow symbols).*

To minimize the difference between our experiments and those reported previously, we subjected the NiTi-Hf balls to severe wear to achieve a geometry similar to a pin and lower contact pressures. The severe wear process entailed using the tribometer to slide the spherical balls on silicon carbide abrasive paper. The wear was allowed to continue until one side of the ball was flattened, as shown in Figure 2. Closer analysis of the flattened region revealed that the edges of the worn region were rounded, effectively corresponding to a much larger radius (see Figure 2c). This rounding is attributable to the fact that the abrasive paper was somewhat compliant, such that the paper wrapped around the edges of the contact during polishing. The effective radii of the flattened balls were determined using a least squares spherical fit to the profiles of the worn balls. The radii of the flattened NiTi-Hf balls created with this method varied from 47.8 to 243 mm. The resultant geometry was similar to the 60NiTi pins used in the previous study and enabled experiments to be performed at much lower Hertz pressures.

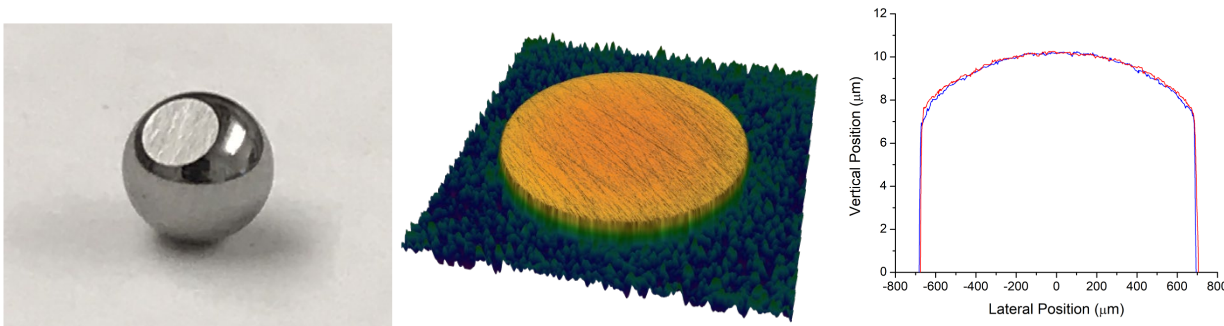

(a) (b) (c)

Figure 2: (a) Photo of a NiTi-Hf *ball after being subjected to severe wear in order to obtain a much larger effective radius for subsequent friction testing. (b) White light interferometer image of the flat region on the ball. (c) Cross-sections of a representative flattened ball showing the large radius produced using the pre-test wear method where the red and blue lines correspond to measurements in two orthogonal directions.*

Friction experiments were run with the flattened balls at a normal load of 30 N, corresponding to a Hertz pressure of 120 +/- 14 MPa. The results are shown in Figure 3. We observe that, although the pressure range and geometry are now comparable to those reported in Ref. [9], our measured friction is still much higher. Also, the friction in our experiments decreases with increasing speed. However, analysis of the balls after flattening indicated that the surface had been roughened by the process. The roughness increased to 257.3 +/- 27.3 nm, where the average and standard deviation were obtained from measurements of the three balls used to obtain the data in Figure 3.

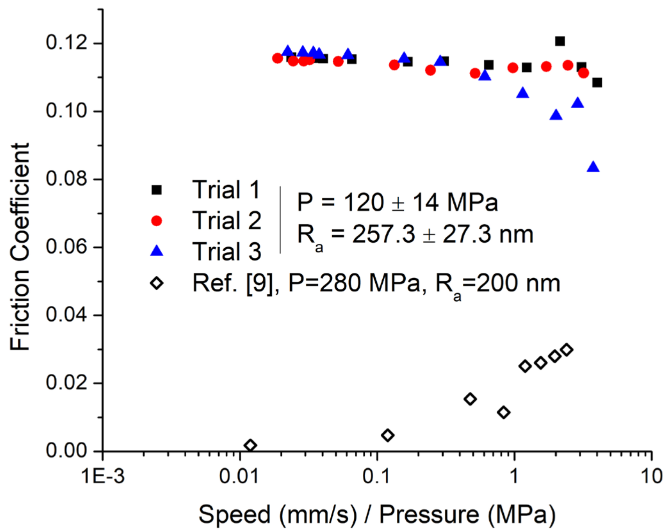

Figure 3: Friction results obtained with flattened NiTi-Hf *balls having large effective radii which enabled much lower pressures to be achieved. Data reported from three independent tests (solid symbols). Also shown are results obtained with a pin-on-flat geometry in Ref. [9] (hollow symbols).*

Since roughening of the balls occurred during the flattening process, additional balls were polished after flattening to create smoother contact surfaces. At this point, there were twelve flattened balls with varying effective radii and roughness. At the constant load of 30 N, the effective radii corresponded to Hertz pressures between 87 and 258 MPa. The average roughness varied from 17.2 to 279.6 nm. Profiles of three representative flattened balls polished to different roughness scales are shown in Figure 4. Each surface was characterized by the average roughness, as well as the root-mean-square roughness (R_q), skewness (S_k), and kurtosis (K_u). A summary of the ball radii and all roughness parameters is given in Table 1. The root-mean-square roughness was larger than the average roughness in all cases, but the trends were the same for both, so only average roughness is reported subsequently. The skewness was slightly below zero for all cases, with an average value of $S_{k,ave}$ = -0.7, indicating surfaces with more valleys than peaks. The kurtosis was larger than three for all cases, with an average value of $K_{u,ave}$=7.6, indicating surfaces with sharper asperities. However, we found no correlation between these two parameters and the observed friction, so they will not be discussed further here.

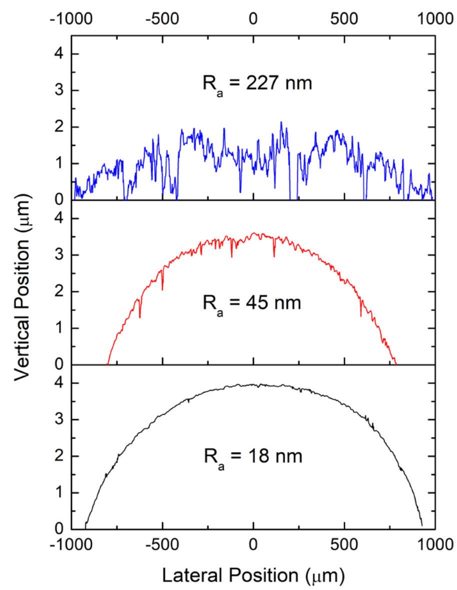

Figure 4: Cross-sections of representative flattened balls polished to different levels of roughness.

Ball	R (mm)	R_a (nm)	R_q (nm)	S_k	K_u
1	47.8	34.9	48.0	-1.0	7.3
2	62.3	17.7	25.3	-0.7	8.0
3	68.9	29.8	39.9	0.0	4.8
4	72.1	39.5	54.2	-0.5	6.4
5	89.9	30.1	40.1	-0.5	5.0
6	99.9	45.4	65.1	-1.5	9.5
7	115.6	17.2	26.5	-0.1	14.2
8	127.6	226.9	313.2	-0.9	7.0
9	138.6	36.4	51.1	-0.7	8.0
10	158.3	279.6	376.2	-0.7	6.2
11	175.2	265.5	366.4	-0.8	7.1
12	243.4	17.7	25.3	-1.0	8.3

Table 1: Effective radius and roughness parameters for twelve flattened balls polished to varying degrees of roughness. Data is sorted by ball radius.

Tests were run for each ball across the same range of speeds reported in Figures 1b and 3. However, to facilitate comparison between the various cases, we focused on the friction at a speed of 31.1 +/- 1.8 mm/s, which is comparable to one of the data points reported in Ref. [9] at 33.4 mm/s. Average friction as a function of effective Hertz pressure for the original three balls (from Figure 1b), the flattened balls, and from Ref. [9] is shown in Figure 5. The friction does not change monotonically with pressure.

However, the roughness of the contacts varied significantly: the original ball roughness was 60.8 +/- 1.6 nm, the flattened ball roughness ranged from 17.2 to 279.6 nm, and the roughness reported in Ref. [9] was 200 nm. Both pressure and roughness can affect the lubrication regime, which determines the friction mechanism, as discussed next.

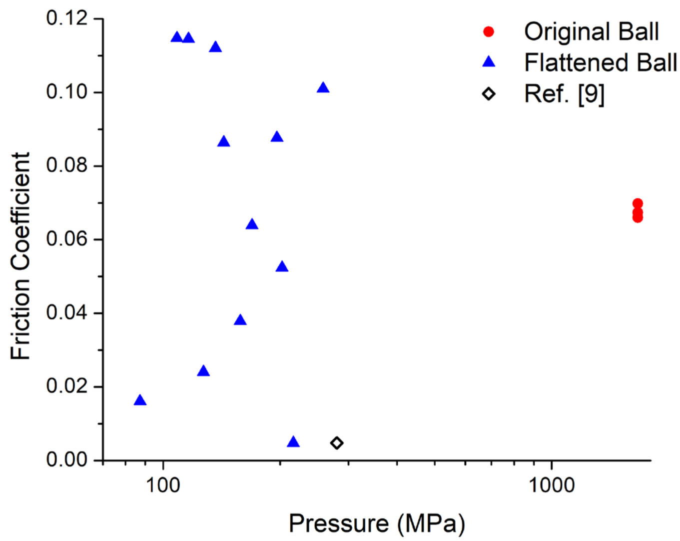

Figure 5: Friction as a function of pressure at constant speed (~31 mm/s) for the original and flattened balls. All tests were performed at a load of 30 N and the pressure varies due to the radius of the flattened ball. Also shown is the result obtained with a pin-on-flat geometry in Ref. [9] (hollow symbol).

In a lubricated contact, surface roughness can determine the lubrication regime based on its magnitude relative to the lubricant film thickness. This can be quantified by the so-called lambda ratio, defined as: $\lambda = h_{min}/\left(R_{a,ball}^2 + R_{a,flat}^2\right)^{1/2}$), where, $R_{a,ball}$ and $R_{a,flat}$ are the average roughness of the two bodies in contact and h_{min} is the minimum film thickness. This parameter has been to estimate the lubrication regime, where $\lambda > 3$ indicates full film lubrication, $1 > \lambda > 3$ suggests mixed lubrication, and $\lambda < 1$ corresponds to boundary lubrication [10]. The minimum film thickness can be estimated using an expression from Hamrock and Dowson [14]:

$$h_{min} = 3.63R\left(\frac{U\eta_0}{ER}\right)^{0.68}(\alpha E)^{0.68}\left(\frac{W}{ER^2}\right)^{-0.073}\left(1 - e^{-0.49k}\right) \qquad (1)$$

For our contact, the effective radius R varies for each flattened ball, the speed U is 31.1 mm/s, the effective elastic modulus E is 164.6 GPa, the pressure-viscosity coefficient α is 15.9 GPa^{-1}, the ambient viscosity η_0 is 0.674 Pa.s, the load W is 30 N, and the ellipticity parameter k is 1 for a spherical geometry.

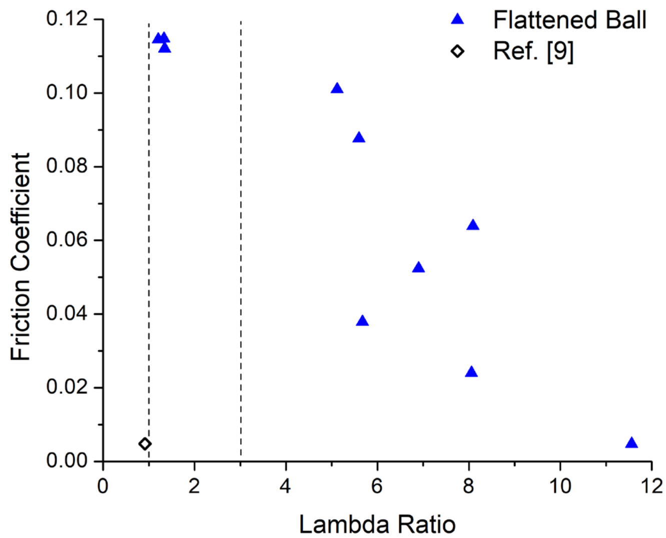

Figure 6: Friction as a function of the λ parameter for the flattened ball tests at ~31 mm/s. Also shown is the result obtained with a pin-on-flat geometry in Ref. [9] (hollow symbol). Vertical dashed lines indicate theoretical transitions between lubrication regimes.

The parameter λ was calculated for all twelve flattened ball cases and the results are shown in Figure 6. The friction decreased with increasing λ. The three tests with λ ~ 1, suggesting nearly boundary lubrication, corresponded to the roughest surfaces ($R_{a,ball}$ = 257.3 +/- 27.3 nm). All other tests had a λ value of greater than 3, indicating full film lubrication. The test that exhibited ultra-low friction (friction coefficient < 0.01) corresponded to a surface roughness of 17.7 nm and therefore λ>10. Therefore, although we measured ultra-low friction, comparable to that reported in Ref. [9], here this result was only achieved with full film lubrication, i.e. not through the action of a protective tribofilm. Using the film thickness calculation described above, the lambda ratio for the data point at comparable speed reported in Ref. [9] is slightly below 1, indicating boundary lubrication. Therefore, we are not able to reproduce or explain the previously-reported superlubricity. Possible explanations include differing geometry and material composition, since our NiTi was alloyed with Hafnium and the large radii were created artificially using severe wear of the balls. We also note that another recent study measured friction with castor oil lubricated 60NiTi and 58Ni39Ti-3Hf and found a minimum achievable friction coefficient of 0.1, much higher than the superlubricity limit [15].

Conclusions

The ability of castor oil to lubricate a NiTi-Hf / steel contacts was evaluated by measuring the friction coefficient in pure sliding conditions under a range of speeds, pressures and surface roughness. With spherical NiTi-Hf balls, it was found that the effect of speed was consistent with that expected based on a traditional Stribeck curve. However, at all speeds, the observed friction was significantly higher than reported in a previous study. To minimize differences between the two studies, the NiTi-Hf balls were subjected to severe wear experiments prior to friction testing in order to achieve lower pressures and geometries comparable to a pin-on-disk experiment. With these flattened balls, friction was still higher than previously-reported. The effect of pressure was explored for a given speed by testing with different flattened ball radii, and it was found that friction did not vary monotonically with pressure. However, measurements with different surface roughness revealed a strong dependence of friction. With the smoothest NiTi-Hf surfaces (R_a~18 nm), ultra-low friction was achieved. However, an analysis of the lambda ratio revealed that this case was likely to be in the full film lubrication regime, where low friction was provided by the fluid entirely supporting the load. Therefore, in contrast to findings of the previous study, it is unlikely that the ultra-low friction observed here was due to the effects of a tribofilm. Regardless, the present study shows that castor oil may be used to lubricate NiTi-Hf bearings, but only if the components are finished to achieve small surface roughness and then maintain that roughness level during operation.

Acknowledgements

The authors thank Dr. Chris DellaCorte at NASA Glenn for generously sharing the NiTi-Hf bearing balls and for research guidance in general. This research was supported by the Merced nanomaterials Center for Energy and Sensing (MACES) through the support of the National Aeronautics and Space Administration (NASA) grant no. NNX15AQ01.

References

[1] Stanford, M. K., Thomas, F., and DellaCorte, C. (2012), “Processing Issues for Preliminary Melts of the Intermetallic Compound 60-NiTiNOL,” Technical Report, NASA/TM-2012-216044.

[2] DellaCorte, C., Noebe, R. D., Stanford, M. K., and Padula, S. A. (2012), "Resilient and Corrosion-proof Rolling Element Bearings Made from Superelastic Ni-Ti Alloys for Aerospace Mechanism Applications," Rolling Element Bearings, STP103887, Y. Takeuchi and W. Mandler, Ed., ASTM International, West Conshohocken, PA, pp. 143-166

[3] DellaCorte, C., Pepper, S.V., Noebe, R., Hull, D.R. and Glennon, G. (2009), “Intermetallic nickel-titanium alloys for oil-lubricated bearing applications,” NASA/TM—2009-215646.

[4] DellaCorte, C. and Glennon, G. (2012), “Ball Bearings Comprising Nickel-Titanium and Methods of Manufacturing Thereof,” U.S. Patent 8182741.

[5] DellaCorte, C. (2014), “Novel Super-Elastic Materials for Advanced Bearing Applications,” Adv. Sci. Tech., **89**, pp. 1-9.

[6] Patila, D., Marinack Jr., M. C., DellaCorte, C., Higgs III, C.F. (2017), “Experimental Investigations of the Superelastic Impact Performance of Nitinol 60,” Tribology Transactions **60**(4), 615–620.

[7] Pepper, S.V. DellaCorte, C., Noebe, R.D. Hull, D.R., Glennon, G. (2009), “Nitinol 60 as a material for spacecraft triboelements,” Proc. 13th European Space Mechanisms and Tribology Symposium – ESMATS 2009, Vienna, Austria.

[8] Pepper, S. V., DellaCorte, C., and Glennon, G. (2010), “Lubrication of Nitinol 60,” Technical Report, NASA/TM-2010-216331.

[9] Zeng, Q-F, Dong, G.-N. and Martin, J. M. (2016), "Green superlubricity of Nitinol 60 alloy against steel in presence of castor oil." Scientific Reports **6**, 29992.

[10] Zeng, Q. F. and Dong, G. N. (2013), “Influence of load and sliding speed on super-low friction of Nitinol 60 alloy under castor oil lubrication.” Trib. Lett. **52**, 47–55.

[11] Zeng, Q. F. and Dong, G. N. (2014), “Superlubricity behaviors of Nitinol 60 alloy under oil lubrication,” Trans. Nonferrous Met. Soc. China **24**, 354-359.

[12] Bongfa, B., Atabor, P. A., Barnabas, A. and Adeoti, M. O. (2015) “Comparison of lubricant properties of Castor oil and commercial engine oil,” Jurnal Tribologi **5**, 1-10.

[13] DellaCorte, C., Stanford, M. K., Jett, T. R. (2015), “Rolling Contact Fatigue of Superelastic Intermetallic Materials (SIM) for Use as Resilient Corrosion Resistant Bearings,” Tribology Letters **57**, 26.

[14] Stachowiak, G. W. and Batchelor, A. W. (1993), “Engineering Tribology,” Elsevier, Amsterdam, Netherlands.

[15] Khanlari, K., Ramezani, M., Kelly, P, Cao, P. and Neitzert, T. (2018), “Comparison of the reciprocating sliding wear of 58Ni39Ti-3Hf alloy and baseline 60NiTi,” Wear **408–409**, 120-130.